Communication

Metal-Mediated Self-Assembly of Protein Superstructures: Influence of Secondary Interactions on Protein Oligomerization and Aggregation

Eric N. Salgado, Richard A. Lewis, Jasmin Faraone-Mennella, and F. Akif Tezcan

J. Am. Chem. Soc., **2008**, 130 (19), 6082-6084 • DOI: 10.1021/ja8012177 • Publication Date (Web): 19 April 2008

J|A|C|S
COMMUNICATIONS

Published on Web 04/19/2008

Metal-Mediated Self-Assembly of Protein Superstructures: Influence of Secondary Interactions on Protein Oligomerization and Aggregation

Eric N. Salgado, Richard A. Lewis, Jasmin Faraone-Mennella, and F. Akif Tezcan*

Department of Chemistry and Biochemistry, University of California, San Diego, 9500 Gilman Drive, La Jolla, California 92093

Received February 18, 2008; E-mail: tezcan@ucsd.edu

Protein−protein interactions (PPIs) are the most diverse of biological self-assembly processes, central to the construction and mechanical integrity of biological machinery, on one hand, and cellular dynamics and communication, on the other. While rational design and control of PPIs would provide access to novel protein assemblies[1] as well as the manipulation of cellular processes,[2,3] such efforts are hampered by the fact that PPIs comprise an extensive set of noncovalent bonds distributed over large and typically noncontiguous molecular surfaces.[4] We have taken on the challenge of controlling PPIs using an inorganic chemical approach. Work by several groups has shown that small organic building blocks with acceptor groups can self-assemble into discrete superstructures and frameworks through metal coordination.[5] We envisioned that the self-assembly of proteins can likewise be controlled by metal binding, with the added complications that (a) protein surfaces are replete with polar side chains capable of coordinating metals, and (b) the interactions between individual proteins—in contrast to those between organic building blocks—may not be negligible. Our previous studies have shown that metal coordination can be largely localized onto multidentate metal binding motifs inserted on surface helices that can outcompete other potential binding sites; one such construct (His^4-cb_{562}; hereafter referred to as MBPC-1, Figure 1) was found to self-assemble into a discrete superstructure upon Zn coordination.[6] In this study, we show that secondary interactions between proteins, that is, those not involving metal coordination, can play a significant role in tuning the oligomerization/aggregation behavior of a protein.

MBPC-1 was engineered with two di-His motifs (59/63 and 73/77) located near each terminus of a single α-helix (helix 3, spanning residues 56−80) in the parent protein cytochrome cb_{562},[7] with the idea that such an arrangement would yield a closed superstructure upon metal coordination. Indeed, at appropriate Zn and protein concentrations, MBPC-1 formed a tetrameric assembly (Zn_4:MBPC-1_4).[6] The crystal structure of Zn_4:MBPC-1_4 revealed a unique quaternary architecture, in which two V-shaped dimers wedged into one another, held together by four Zn ions with identical His^3(63/73/77)−Asp^1(74) coordination environments (Figure 2a). The key to this supramolecular arrangement was the Asp74 residue located within the His73/77 clamp: Zn coordination by Asp74—rather than His59—allowed the V-shaped dimers and, ultimately, the observed tetramer to be formed (Figure S1). Hydrodynamic measurements showed that MBPC-1 did not have a tendency to self-associate in the absence of metals, which indicated that metal binding was the driving force for oligomerization. At the same time, the tetramer was found to have an extensive PPI surface area of nearly 5000 Å^2, raising the possibility that

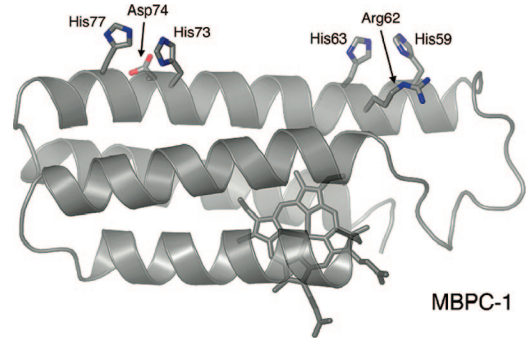

Figure 1. Structure of MBPC-1 (based on the monomeric building blocks of the Zn_4:MBPC-1_4 assembly; PDB ID: 2QLA).

secondary interactions between proteins may still influence the formation of the observed tetramer. If, on the other hand, these interactions had negligible effect and metal coordination was the sole determinant of the supramolecular geometry, then the whole oligomeric assembly could be "inverted" simply by moving the coordinating Asp residue from within the His73/77 motif at the C-terminal end of helix 3 to the N-terminus, inside the His59/63 motif (Figure 1). Thus, we engineered MBPC-2, the D74A/R62D variant of MBPC-1 (its approximate mirror image in terms of metal coordination) and determined its Zn-induced self-assembly properties.

As planned, MBPC-2 forms tetramers upon addition of 1 molar equiv of Zn according to sedimentation velocity (SV) and sedimentation equilibrium (SE) measurements (Supporting Information; see also Figure 4). These experiments indicate that the stability of Zn_4:MBPC-2_4 is elevated compared to Zn_4:MBPC-1_4, with apparent association constants significantly higher than the latter.[8] Zn_4:MBPC-2_4 readily lent itself to crystallization, and we determined its structure at 1.9 Å resolution (PDB ID: 3C62). The Zn_4:MBPC-2_4 architecture is similar to that of Zn_4:MBPC-1_4, with two interlaced V-shaped dimers that are slightly more open, an overall topology that is slightly flatter, and a nearly identical buried protein surface area (∼5000 Å^2) (Figure 2). The Zn_4:MBPC-2_4 structure is indeed the "inverse" of Zn_4:MBPC-1_4 (Figure 2a). Whereas the V-shapes are joined at the helix 3 C-termini in the latter, they are cross-linked at the N-terminus in the former; the transition between the two superstructures resembles a scissor motion. Surprisingly, Asp62 is not involved in Zn binding. Instead, each of the four Zn ions in the assembly are ligated by the His73/77 motif from one monomer, His59 from a second, and His63 from a third, yielding an ideal tetrahedral His^4−Zn coordination geometry with an average Zn−His bond distance of 2.05 Å

10.1021/ja8012177 CCC: $40.75

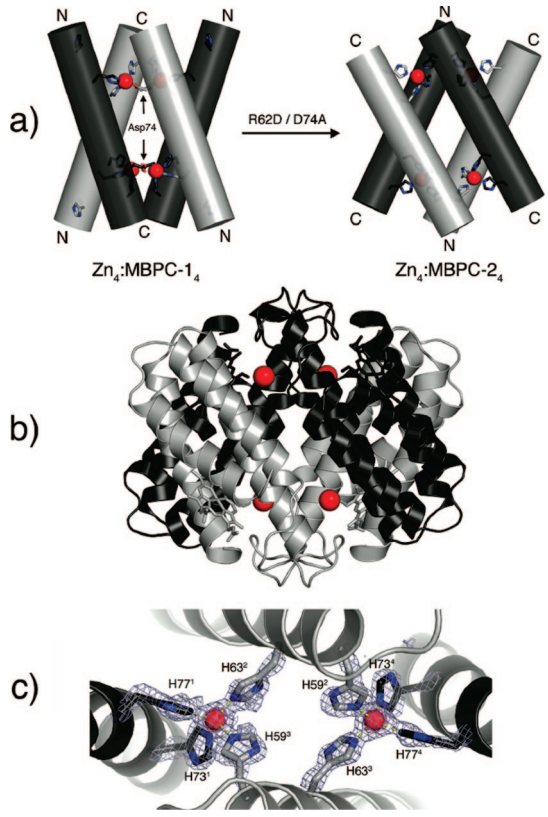

Figure 2. (a) Cylindrical representations of Zn_4:MBPC-1_4 and Zn_4:MBPC-2_4 helix 3's and side chains involved in Zn coordination, viewed along the noncrystallographic 2-fold symmetry axis. Pairs of protein molecules that form the V-shaped dimers are colored alike. The N- and C-termini of the four helix 3's in each assembly are labeled accordingly. (b) Ribbon representation of the Zn_4:MBPC-2_4 crystal structure. (c) Close-up view of the Zn coordination environment down the noncrystallographic 2-fold symmetry axis and the corresponding simulated annealing F_o-F_c omit electron density map (3.5σ).

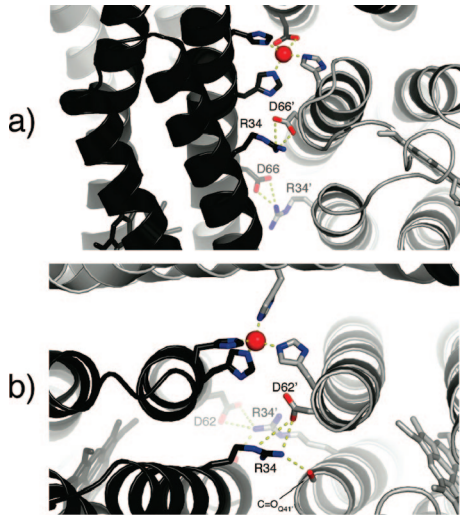

Figure 3. Interfacial H-bonding interactions in Zn_4:MBPC-1_4 (a) and Zn_4:MBPC-2_4 (b) assemblies that involve R34 and D66 in the former and R34 and D62 in the latter. The pairwise interactions shown above are repeated twice due to the internal 2-fold symmetry of each tetrameric assembly.

(Figure 2c). In this arrangement, each V-shape is stabilized by His59 and His63 coordination—instead of the expected Asp62 and His63 coordination—from two monomers, which splay apart

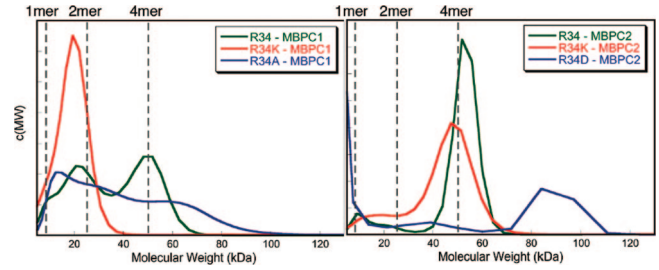

Figure 4. Molecular weight distributions of MBPC-1 (left) and MBPC-2 (right) species as determined by sedimentation velocity measurements. All samples contain 600 μM protein and 600 μM Zn, with the exception of R34A-MBPC-1, which contains 300 μM Zn.[13]

to bind two Zn ions, thereby joining the helix 3 N-termini together. Interestingly, His^4-Zn coordination has rarely been observed in natural systems, one example being the HAP1 transcriptional factor that contains a structural $His^2(N\epsilon)$, $His^2(N\delta)-Zn$ site.[9] Utilizing metal-binding motifs on surfaces to nucleate PPIs may provide access to unusual coordination environments not favored within protein interiors.[10]

While similarities between Zn_4:MBPC-1_4 and Zn_4:MBPC-2_4 structures suggest convergence in their mechanisms of self-assembly (vide infra), the differences in their metal coordination modes raise some questions: Why does MBPC-2 not oligomerize through the His^3-Asp^1 Zn coordination motif although it has access to it? Conversely, why does MBPC-1 not self-assemble through the same His^4 motif as MBPC-2? And finally, why is Zn_4:MBPC-2_4 more stable than Zn_4:MBPC-1_4 despite the fact that both assemblies are held together by four Zn ions in unstrained, tetrahedral coordination geometries? We thus decided to take a closer look at the protein interfaces in both assemblies to determine whether secondary interactions may influence metal-induced self-assembly. As expected from a soluble protein whose surface is not optimized for self-association, the interfaces in both Zn_4:MBPC-1_4 and Zn_4:MBPC-2_4 structures feature overwhelmingly polar residues that are poorly packed. Furthermore, there are surprisingly few interfacial H-bonding interactions given the extensive buried protein surfaces in both assemblies. Earlier surveys of oligomeric protein structures have indicated average interfacial H-bond densities ranging from 0.5 to 0.7 per 100 $Å^2$ of buried surface;[11,12] these values are considerably higher than 0.3 and 0.2 per 100 $Å^2$ observed in Zn_4:MBPC-1_4 and Zn_4:MBPC-2_4 complexes. Significantly, the majority of these H-bonding interactions involve two pairs of residues that form salt bridges: Arg34−Asp62 in Zn_4:MBPC-2_4 accounting for 9 out of a total of 15 interactions, and Arg34−Asp66 in Zn_4:MBPC-1_4 accounting for 7 out of a total of 10 (Figure 3 and Table S2).

In order to probe the possible role of these salt bridges in the self-assembly of the two tetramers, we generated a series of Arg34 mutants of MBPC-1 and MBPC-2 aimed at weakening or abolishing these interactions. Figure 4 shows the oligomerization behavior of the Arg34 variants as determined by sedimentation velocity experiments. Indicating the higher relative stability of the Zn_4:MBPC-2_4, the parent MBPC-2 molecule exists only in the tetrameric form at 600 μM protein and Zn concentrations, whereas a significant population of dimeric species is also present with MBPC-1 under the same conditions. Upon the mutation of Arg34 to the shorter Lys, the peak for the tetrameric assembly disappears entirely for MBPC-1 and becomes broader for MBPC-2, consistent with the weakening of the salt-bridging interaction. The 1.75 Å crystal structure of

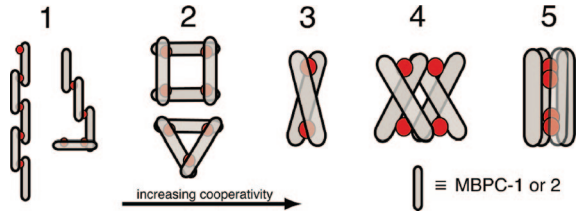

Figure 5. Possible Zn-induced oligomerization states of MBPC-1 and -2 under limiting (≤1 equiv) metal concentrations assuming a four-coordinate Zn geometry. (1) extended structures/aggregates, (2) trimer or tetramer with His^4 coordination shared by two monomers, (3) dimer with His^4 coordination shared by two monomers, (4) tetramer with His^4 or His^3−Asp coordination shared by three monomers, and (5) tetramer with His^4 coordination shared by four monomers.

the Zn_4:(R34K)MBPC-2_4 assembly (PDB ID: 3C63) reveals that Lys34 indeed maintains the salt bridge to Asp62 and stabilizes the parent tetrametric assembly, but its interactions are not as extensive compared to those of Arg34 (Figure S2). Dramatically, when Arg34 is mutated to Ala and Asp in MBPC-1 and MBPC-2, respectively, the tetrameric forms are replaced by heterogeneous ensembles that contain higher order aggregates.[13] These findings demonstrate that Arg34 interactions clearly are the guiding factor for the metal-induced oligomerization of MBPC-1 and -2.

In the presence of limiting amounts of Zn, MBPC-1 or MBPC-2 molecules likely sample all of the conformations depicted in Figure 5, with the possible exception of **5** due to steric reasons. While monomeric and dimeric (**3**) forms dominate at low protein concentrations, the tetrameric, interlaced conformation **4** with the highest Zn-binding cooperativity is expected to be the prevalent species at intermediate concentrations. This is indeed borne out by the structural convergence of Zn_4:MBPC-1_4 and Zn_4:MBPC-2_4 assemblies despite differences in their metal coordination modes. Secondary interactions, particularly those involving Arg34, then, are crucial for fine-tuning the relative stabilities and geometric specificities of the different oligomeric states. MBPC-1 exclusively forms the type **4** conformation with the observed His^3−Asp coordination motif rather than the His^4 motif seen in Zn_4:MBPC-2_4 because (a) the Arg34−Asp66 interaction (Figure 3a) stabilizes the former geometry, and (b) the latter geometry would align the original Arg62 in MBPC-1 across from Arg34 (Figure 3b), leading to a destabilizing effect. Conversely, MBPC-2 specifically forms the type **4** conformation with His^4 coordination as opposed to the His^3−Asp motif because it is energetically more favorable to utilize Asp62 in an interfacial salt bridge when a tetracoordinate Zn geometry is already accessible with four histidines. Last, a broader inspection of the interfaces in Zn_4:MBPC-1_4 and Zn_4:MBPC-2_4 reveals that the former assembly features a higher number of unfavorable interactions and side chain environments (Supporting Information), which attests to its lower stability.[14]

To what extent H-bonds and salt bridges contribute to the stability of proteins and PPIs can greatly vary from system to system.[15] Yet, it is generally thought that these alignment-dependent interactions are important in limiting the number of possible low energy docking conformations, thus playing a major role in determining specificity.[16,17] Our results provide clear evidence that salt-bridging and H-bonding interactions can dictate the geometric alignment of protein partners, leading to the population of discrete supramolecular structures over other conformations of similar energy. The combined ability to direct PPIs through metal coordination and secondary interactions could provide the specificity required for the construction of complex, multicomponent protein superstructures and the selective control of cellular processes that involve protein−protein association reactions.

Acknowledgment. We thank Drs. Arnold L. Rheingold and Antonio DiPasquale for their help with X-ray data collection, and Drs. Andrew Herr, Peter Schuck, Patrick Brown, and Xavier Ambroggio for helpful discussions. This work was supported by UCSD, a Hellman Faculty Scholar Award (F.A.T.), NIH (Molecular Biophysics Training Grant GM08326 to E.N.S.), and NSF (Instrumentation Grant 0634989 to A.L.R.).

Supporting Information Available: Materials and methods for protein expression/purification/characterization, experimental details for sedimentation velocity/equilibrium and NMR measurements, crystallographic data and collection/refinement statistics, table for interfacial interactions. This material is available free of charge via the Internet at http://pubs.acs.org.

References

(1) Grueninger, D.; Treiber, N.; Ziegler, M. O. P.; Koetter, J. W. A.; Schulze, M. S.; Schulz, G. E. *Science* **2008**, *319*, 206–209.
(2) Shifman, J. M.; Mayo, S. L. *J. Mol. Biol.* **2002**, *323*, 417–423.
(3) Reina, J.; Lacroix, E.; Hobson, S. D.; Fernandez-Ballester, G.; Rybin, V.; Schwab, M. S.; Serrano, L.; Gonzalez, C. *Nat. Struct. Biol.* **2002**, *9*, 621–627.
(4) (a) Kortemme, T.; Baker, D. *Curr. Opin. Chem. Biol.* **2004**, *8*, 91–97. (b) Moreira, I. S.; Fernandes, P. A.; Ramos, M. J. *Proteins* **2007**, *68*, 803–812. (c) Shoemaker, B. A.; Panchenko, A. R. *PLoS Comput. Biol.* **2007**, *3*, 595–601. (d) Fletcher, S.; Hamilton, A. D. *J. R. Soc. Interface* **2006**, *3*, 215–233.
(5) (a) Fujita, M.; Tominaga, M.; Hori, A.; Therrien, B. *Acc. Chem. Res.* **2005**, *38*, 369–378. (b) Banerjee, R.; Phan, A.; Knobler, C.; Furukawa, H.; O'Keeffe, M.; Yaghi, O. M. *Science* **2008**, *319*, 939–943. (c) Caulder, D. L.; Raymond, K. N. *Acc. Chem. Res.* **1999**, *32*, 975–982. (d) Holliday, B. J.; Mirkin, C. A. *Angew. Chem., Int. Ed.* **2001**, *40*, 2022–2043. (e) Leininger, S.; Olenyuk, B.; Stang, P. J. *Chem. Rev.* **2000**, *100*, 853–907.
(6) Salgado, E. N.; Faraone-Mennella, J.; Tezcan, F. A. *J. Am. Chem. Soc.* **2007**, *129*, 13374–13375.
(7) Faraone-Mennella, J.; Tezcan, F. A.; Gray, H. B.; Winkler, J. R. *Biochemistry* **2006**, *45*, 10504–10511.
(8) The SE data were satisfactorily fit to a monomer/dimer/tetramer association model. The apparent monomer/dimer and dimer/tetramer dissociation constants ($-\log K_d$) are 4.9 and 4.8 M for Zn_4:MBPC-1_4, and 11.9 and 9.15 M for Zn_4:MBPC-2_4, respectively. These numbers, however, should not be taken as "true" dissociation constants because the Zn−protein binding equilibria are also contained within. While Zn_4:MBPC-2_4 is clearly more stable than Zn_4:MBPC-1_4, as indicated in Figure 4, the differences in their dissociation constants are likely inflated by the cooperative nature of Zn binding and protein association.
(9) King, D. A.; Zhang, L.; Guarente, L.; Marmorstein, R. *Nat. Struct. Biol.* **1999**, *6*, 64–71.
(10) Unusual metal coordination environments also have been obtained within de novo designed coiled-coil architectures. See for example: Matzapetakis, M.; Farrer, B. T.; Weng, T. C.; Hemmingsen, L.; Penner-Hahn, J. E.; Pecoraro, V. L. *J. Am. Chem. Soc.* **2002**, *124*, 8042–8054.
(11) Janin, J.; Miller, S.; Chothia, C. *J. Mol. Biol.* **1988**, *204*, 155–164.
(12) Jones, S.; Thornton, J. M. *Proc. Natl. Acad. Sci. U.S.A.* **1996**, *93*, 13–20.
(13) Upon addition of equimolar Zn (600 μM), (R34A)MBPC-1 promptly precipitates out of solution, indicating formation of high-order aggregates.
(14) Another manifestation of the lower stability of Zn_4:MBPC-1_4 is its higher sensitivity to R34 mutations.
(15) (a) Froloff, N.; Windemuth, A.; Honig, B. *Protein Sci.* **1997**, *6*, 1293–1301. (b) Makhatadze, G. I.; Loladze, V. V.; Ermolenko, D. N.; Chen, X. F.; Thomas, S. T. *J. Mol. Biol.* **2003**, *327*, 1135–1148. (c) Kumar, S.; Nussinov, R. *Biophys. J.* **2002**, *83*, 1595–1612.
(16) Hendsch, Z. S.; Tidor, B. *Protein Sci.* **1994**, *3*, 211–226.
(17) Sheinerman, F. B.; Norel, R.; Honig, B. *Curr. Opin. Struct. Biol.* **2000**, *10*, 153–159.

JA8012177